Hypersonic Laminar Wakes and Transition Studies

ADRIAN PALLONE,* JOHN ERDOS,† AND JEROME ECKERMAN‡
Avco Corporation, Wilmington, Mass

This report presents the results of theoretical and experimental investigations of the flow in the wake of hypersonic vehicles Nonsimilar solutions of the equations governing the "far wake" are obtained, and numerical results for the flow field in the wake of ballistic range and wind-tunnel models and of a flight-size vehicle are presented A series of ballistic range experiments with conical models of 10°, 15°, and 27½° semivertex angles are described The model velocity ranges between 4000 and 17,000 fps with range pressures varying from 15 to 330 mm of Hg in air The experimental data are discussed in detail, and the analysis is used to compute and correlate appropriate transition parameters Based on the correlation, exemplary predictions of the location of transition in the wake of a 12° semivertex angle cone at 22,000 fps are made for the altitude range from 200,000 to 100,000 ft

Nomenclature

d = base diameter of body
h = static enthalpy
H = stagnation enthalpy
j = an index, either 0 or 1
M = Mach number
p = pressure
Pr = Prandtl number
r,y = normal coordinate, measured from axis or plane of symmetry
R = gas constant
Re_x = Reynolds number, based on local inviscid properties and x distance
S = Sutherland constant
T = static temperature
u = x component of velocity
v = r component of velocity
V = velocity vector
x = streamwise coordinate, measured from forward stagnation point
ρ = mass density
μ = viscosity
ξ = transformed streamwise coordinate
η = transformed normal coordinate
δ = wake thickness (from axis or plane of symmetry)
θ = momentum thickness
ϕ = cone semivertex angle
γ = ratio of specific heats

Subscripts

1 = evaluated at $r = \delta$ or $\eta = 1$
c = evaluated at $r = 0$ or $\eta = 0$
k = evaluated at edge of kth strip
x,r,η = partial derivative with respect to variable indicated
0 = reservoir conditions

I Introduction

THE flow in the wake of hypersonic vehicles has been the subject of considerable research in recent years The interest in this subject stems mainly from the realization that the trails of hypersonic vehicles are a potentially significant source of observables, i e , electrons and radiating species The bulk of the literature deals mainly with the trails of blunt bodies[1-3] where the viscous core comprises a significant portion of the wake flow field (from the point of view of observables) only if turbulent mixing is present However, in the case of slender bodies (e g , Fig 1) the observables in the inviscid flow field are minimized, and the viscous region (laminar or turbulent) becomes the sole source of electrons and radiating species

Excellent accounts of the state of the art of the turbulent far wake have been presented by Lees[4] and Vaglio-Laurin, Bloom, and Byrne[5] These authors extended their blunt-body analyses to the slender-body case Most analyses of the laminar far wake have been restricted to similar solutions involving linearized forms or to solutions obtained by the Karman-Pohlhausen method The notable exception is the classical Goldstein solution for the incompressible wake of a flat plate[6]

Recent experimental data acquired at Avco/RAD and the Naval Ordinance Laboratory (NOL) ballistic ranges show appreciable lengths of laminar wake at Reynolds numbers higher than those previously reported[4] Therefore, for slender bodies a critical analysis of the laminar far wake has a twofold value: to provide detailed flow fields for the prediction of observables, and to compute accurately the appropriate transition parameters

This paper presents a theoretical analysis of the laminar far wake and also contains some of the experimental results obtained in the Avco/RAD ballistic range The method of analysis is an extension of the multistrip integral technique for obtaining nonsimilar solutions of the laminar boundary-layer equations[7] Since no solution of the near wake is presently available, the choice of initial conditions is somewhat arbitrary However, initial velocity and enthalpy profiles can be prescribed with some degree of confidence from existing knowledge of gross near-wake properties and by utilizing over-all momentum and energy conservation Only wakes composed of pure air in equilibrium or completely frozen are considered in the present analysis Some results for nonequilibrium wakes have been obtained by Vaglio-Laurin, Bloom, et al by the Karman-Pohlhausen technique[3,5,8] An analysis using the present nonsimilar technique has been formulated for chemical nonequilibrium and some preliminary results obtained,[9,10] but they are not included here

II Analysis

Steady flow downstream of the neck of a wake (i e , the stagnation point in the wake beyond which no recirculation

Presented as Preprint 63-171 at the AIAA Summer Meeting, Los Angeles, Calif , June 17–20, 1963; revision received February 24, 1964 This work was supported by the Air Force Ballistic Systems Division under contract AF04(694)-239 The authors wish to acknowledge William McKay for his valuable contributions to the experimental phase of this study, and Doris Page for her excellent work in preparing this manuscript

* Section Chief, Experimental and Theoretical Aerodynamics Section, Research and Advanced Development Division

† Senior Scientist, Experimental and Theoretical Aerodynamics Section, Research and Advanced Development Division Member AIAA

‡ Group Leader, Ballistic Range, Research and Advanced Development Division Member AIAA

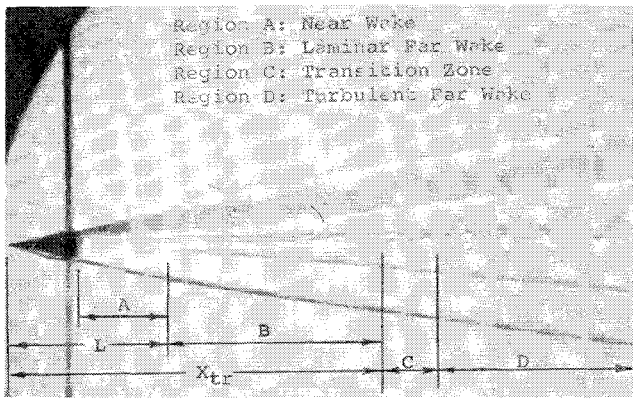

Fig 1 Typical features of a slender body flow field (10° cone, V_∞ = 9700 fps, 0 300-in base diameter, P_∞ = 75 mm Hg)

takes place) can be described in the context of boundary-layer theory by

$$(\rho u r^j)_x + (\rho v r^j) = 0 \tag{1}$$

$$\rho u u_x + \rho v u_r = -p_x + r^{-j}(\mu r^j u_r) \tag{2a}$$

$$0 = p_r \tag{2b}$$

$$\rho u H_x + \rho v H = r^{-j}\{(\mu r^j/Pr)[H + (Pr - 1)(u^2/2)]\} \tag{3}$$

where

$$j = \begin{cases} 0 \text{ for planar flow} \\ 1 \text{ for axisymmetric flow} \end{cases}$$

The conventional boundary conditions apply at the outer edge of the wake:

$$\left.\begin{aligned} u &= u_1,\ u_r = 0 \\ H &= H_1,\ H_r = 0 \end{aligned}\right\} \text{ at } r = \delta$$

whereas at the plane, or axis of symmetry, the boundary conditions are

$$\left.\begin{aligned} u &= u_r,\ u = 0 \\ H &= H_r,\ H_r = 0 \end{aligned}\right\} \text{ at } r = 0$$

In the present analysis, the wake is divided into an arbitrary number of strips N in the streamwise direction, and the equations are then integrated with respect to r across the strips, i e , between the limits of $r = 0$ and $r = r_k$, to give two ordinary differential equations§:

$$\frac{d}{dx}\left[\rho_1 u_1^2 \int_0^{r_k} \frac{\rho u}{\rho_1 u_1}\left(\frac{u_k}{u_1} - \frac{u}{u_1}\right) r^j dr\right] - \rho_1 u_1^2 \left(\int_0^{r_k} \frac{\rho u}{\rho_1 u_1} r^j dr\right) \frac{d}{dx}\left(\frac{u_k}{u_1}\right) - \rho_1 u_1 u_k \left(\int_0^{r_k} \frac{\rho u}{\rho_1 u_1} r^j dr\right) \frac{d}{dx}(\ln u_1) - \frac{dp}{dx}\int_0^{r_k} r^j dr + \left[u_1 \mu r^j \left(\frac{u}{u_1}\right)\right]_0^{r_k} = 0 \tag{4}$$

$$\frac{d}{dx}\left[\rho_1 u_1 \int_0^{r_k} \frac{\rho u}{\rho_1 u_1}\left(\frac{H_k}{H_1} - \frac{H}{H_1}\right) r^j dr\right] - \rho_1 u_1 \left(\int_0^{r_k} \frac{\rho u}{\rho_1 u_1} r^j dr\right) \frac{d}{dx}\left(\frac{H_k}{H_1}\right) + \left\{\frac{\mu r^j}{Pr}\left[\left(\frac{H}{H_1}\right) + (Pr - 1)\frac{u_1^2}{2H_1}\left(\frac{u}{u_1}\right)^2\right]\right\}_0^{r_k} = 0 \tag{5}$$

§ The strip-integral method is discussed in greater detail in Ref 7

The transformed independent variables ξ, η, are now introduced:

$$\xi = x/L$$

$$\eta = \left[\frac{(j+1)}{\delta_t^{j+1}} \int_0^r \frac{\rho}{\rho_1} r^j dr\right]^{1/(j+1)}$$

where L is a characteristic length of the problem and

$$\delta_t = \left[(j+1)\int_0^\delta \frac{\rho}{\rho_1} r^j dr\right]^{1/(j+1)}$$

is the thickness of the velocity and thermal profiles in the transformed plane The equations now become

$$\left(\frac{j+1}{2}\right) F_{1k}\frac{d\lambda}{d\xi} + \lambda\frac{dF_{1k}}{d\xi} - \lambda F_{2k}\frac{d}{d\xi}\left(\frac{u_k}{u_1}\right) + \left[\frac{2F_{3k}}{\eta_k}\left(\frac{\mu_1}{\rho_1 u_1 L}\right)^{1/2}\right]^j (l_k\tau_k - l\tau) + \lambda\left[F_{1k}\frac{d}{d\xi}\ln(\rho_1 u_1 \mu_1)^{1/2} + \left(F_{1k} - \frac{u_k}{u_1}F_{2k} + F_{3k}\right)\frac{d\ln u_1}{d\xi}\right] = 0 \tag{6}$$

$$\left(\frac{j+1}{2}\right) F_{4k}\frac{d\lambda}{d\xi} + \lambda\frac{dF_{4k}}{d\xi} - \lambda F_{2k}\frac{d}{d\xi}\left(\frac{H_k}{H_1}\right) + \left[\frac{2F_{3k}}{\eta_k}\left(\frac{\mu_1}{\rho_1 u_1 L_1}\right)^{1/2}\right]^j \left\{\frac{l_k}{Pr}\left[\sigma_k + \frac{u_1^2}{H_1}(Pr - 1)\frac{u_k}{u_1}\tau_k\right] - \frac{l_e}{Pr}\left[\sigma + \frac{u_1^2}{H_1}(Pr - 1)\frac{u_e}{u_1}\tau\right]\right\} + \lambda F_{4k}\frac{d}{d\xi}\ln(\rho_1 u_1 \mu_1)^{1/2} = 0 \tag{7}$$

where

$$\lambda = \left(\frac{\rho_1 u_1 L}{\mu_1}\right)^{1/(j+1)}\left(\frac{\delta_t}{L}\right)^2$$

$$\tau = \left(\frac{u}{u_1}\right)_\eta$$

$$\sigma = \left(\frac{H}{H_1}\right)_\eta$$

$$l = \frac{\rho\mu}{\rho_1\mu_1}$$

$$\eta_k = \frac{1 + (N - k)}{N}$$

$$F_{1k} = \int_0^{\eta_k} \frac{u}{u_1}\left(\frac{u_k}{u_1} - \frac{u}{u_1}\right)\eta^j d\eta$$

$$F_{2k} = \int_0^{\eta_k} \frac{u}{u_1}\eta^j d\eta$$

$$F_{3k} = \int_0^{\eta_k} \frac{\rho_1}{\rho}\eta^j d\eta$$

$$F_{4k} = \int_0^{\eta_k} \frac{u}{u_1}\left(\frac{H_k}{H_1} - \frac{H}{H_1}\right)\eta^j d\eta$$

$$k = 1,2\,3 \quad , N$$

The transformed boundary conditions are

$$\left.\begin{aligned} u/u_1 &= 1,\ \tau = 0 \\ H/H_1 &= 1,\ \sigma = 0 \end{aligned}\right\} \text{ at } \eta = 1,$$

$$\left.\begin{aligned} u/u_1 &= u_r/u_1,\ \tau = 0 \\ H/H_1 &= H_r/H_1,\ \sigma = 0 \end{aligned}\right\} \text{ at } \eta = 0$$

Moreover, the transformed momentum and energy equations

evaluated at $\eta = 0$ become

$$\frac{u_c}{u_1}\frac{d}{d\xi}\left(\frac{u_c}{u_1}\right) - \frac{(j+1)l_c\tau_{\eta c}}{\lambda(\rho/\rho_1)^j(\rho_1 u_1 L/\mu_1)^{j/2}} - \left[\frac{\rho_1}{\rho} - \left(\frac{u_c}{u_1}\right)^2\right]\frac{d\ln u_1}{d\xi} = 0 \quad (8)$$

and

$$\frac{u_c}{u_1}\frac{d}{d\xi}\left(\frac{H_c}{H_1}\right) - \frac{(j+1)l_c}{\lambda(\rho/\rho_1)^j(\rho_1 u_1 L/\mu_1)^{j/2}} \times \left\{\sigma_\eta + (Pr-1)\frac{u_1^2}{H_1}\left(\frac{u_c}{u_1}\right)\tau_{\eta c}\right\} = 0 \quad (9)$$

The velocity and stagnation enthalpy profiles can be expressed as polynominals in η However, additional numerical accuracy can be obtained by choosing the following¶:

$$\frac{u}{u_1} = 1 + e^{-\eta/(1-\eta)}\sum_{n=0}^{N} a_n\eta^n$$

$$\frac{H}{H_1} = 1 + e^{-\eta/(1-\eta)}\sum_{n=0}^{N+1} b_n\eta^n$$

which identically satisfy the imposed boundary conditions at $\eta = 1$ (and moreover satisfy the requirement that all higher-order derivatives also vanish at that point) The polynominal coefficients are made to satisy the boundary conditions at $\eta = 0$ and the values of u_k and H_k at the strip boundaries and at the wake axis, or plane, of symmetry

The ordinary equation of state, $p = \rho RT$, provides the necessary thermodynamic relations for a perfect gas with frozen flow approximated by the use of the appropriate gas constant R and ratio of specific heats γ A Mollier chart is employed for the thermodynamics of equilibrium air

At low temperatures, the Sutherland viscosity law is employed to give

$$l_k = \left(\frac{T_k}{T_1}\right)^{1/2}\left[\frac{1 + S/T_1}{T_k/T_1 + S/T_1}\right] \qquad (k = 1,2,3, \quad , N,c)$$

where $S = 120°\text{K}$, whereas at high temperatures the (equilibrium) $\rho\mu$ ratio is approximated by

$$l_k = \frac{A(h_k/h_r)^{-1/2} - B(h_k/h_r)^{-1}}{A(h_1/h)^{-1/2} - B(h_1/h)^{-1}} \qquad (k = 1,2,3, \quad , N,c)$$

where $A = 3\,03$, $B = 2\,03$, $h = 4\,5 \times 10^6\ \text{ft}^2/\text{sec}^2$ Therefore, $2N + 2$ first-order ordinary differential equations are obtained (N momentum integral, N energy integral, and momentum and energy at $r = 0$) which can be solved numerically for the $2N + 2$ unknowns (λ, u_k, H_k, for $k = 2, 3, \quad , N$, and u , H , and $H_{\eta\eta}$) A predictor-corrector marching scheme[11] is employed for solution of the equations on an IBM 7094 **

III Hypersonic Laminar Far Wake for a Slender Body

A Initial (Neck) Conditions

The conditions that occur at the neck of the hypersonic wake are the result of simultaneous mixing and recirculation of the boundary-layer shed from the body, as well as a strong adverse pressure gradient (which "drives" the recirculating flow) Also at the base of the body is a stagnation point that has been experimentally observed to have many of the features (e g , high heat flux) of a blunt-body stagnation point, although less severe Unfortunately, the near wake thus far has eluded successful theoretical treatment, but it is currently receiving considerable attention Various approximations have been attempted, but none offer any really satisfactory insight into the mechanism or magnitude of the recirculation and base heating

The mixing phenomenon per se has been treated by Denison and Baum,[12] and Vaglio-Laurin, Bloom, and Byrne[5] as an extension of the earlier ideas of Chapman,[13] who studied the mixing of a stream with quiescent air Chapman's analysis assumed a zero-thickness shear layer at the beginning of the mixing region, for which he obtained a value of $u_d/u_1 = 0\,587$ for the velocity ratio of the dividing streamline †† Denison and Baum considered the supersonic mixing process starting with a Blasius profile and both cold quiescent air (freestream static temperature) and hot quiescent air (freestream stagnation temperature) for a variety of cone and wedge angles Their results indicate that the dividing streamline velocity ratio is on the order of 0 25 to 0 20 at hypersonic speeds for 10° to 20° cones for the cold case, and 0 35 to 0 30 for the hot case With constant-temperature quiescent air (at approximately the body wall temperature), constant pressure mixing, and Prandtl number of unity, the Crocco integral is an exact solution of the energy equation, which gives

$$H_d/H_1 = [1 - (H_b/H_1)](u_d/u_1) + (H_b/H_1)$$

where

H_d = dividing streamline total enthalpy
H_b = total enthalpy of the quiescent air
H_1 = total enthalpy of the inviscid stream

For the cold case, $H_b/H_1 \ll 1$, giving $H_d/H_1 \approx u_d/u_1$ Clearly, in the hot case $H_d/H_1 \approx 1$ Therefore, consideration of the mixing process alone leads to a realistic lower limit on the dividing streamline enthalpy Assuming that the compression process occurs through a shock-like discontinuity (allowing the neglect of viscous dissipation), then the dividing streamline enthalpy can be taken as the value occurring on the axis at the neck (i e , where the dividing streamline is stagnated)

The nature of the compression process in the neck region suggests that the neck bears certain similarities to a boundary-layer separation point (Indeed, it has been recognized by various authors that gross properties, such as base pressure and wake angle, are predictable in terms of separation-point pressure correlations) Therefore, the use of a separation-point velocity profile from similarity solutions such as Cohen and Reshotko[14] appears to be a reasonable approximation However, the enthalpy profile that would result after such a compression is not known beyond the axis value indicated previously Clearly, the use of the Crocco integral is not correct for the entire near wake, a region which includes strong pressure gradients, but it does have the justification of being at least a consistent means of approximating the neck enthalpy profile in terms of the assumed velocity profile and the (approximately) known enthalpy on the axis However, it should be noted that the use of the Crocco integral leads to an "annulus" of high-temperature gas, rather than a "cylinder," at the neck for slender bodies It is not obvious whether or not this is physically reasonable; intuitively it would be expected that the peak temperature would occur at the axis Regardless, for the lack of any better knowledge

¶ However, a posteriori, with four to six strips, the results become independent of the type polynomial expression selected

** It is important to note that in a numerical solution Eqs (8) and (9) are singular for $u = 0$, although, as pointed out by Kubota,[24] this difficulty can be avoided in an analytical solution by use of an appropriate, nonzero pressure gradient The behavior of the equations near this rear stagnation point has been examined by Cheng[25] and by Vaglio-Laurin, Bloom, and Byrne[5] In the present analysis, solution of the equations is always begun slightly away from the stagnation point, with a small but finite value of u

†† The "streamline" that separates the net recirculating mass flux from that which continues downstream past the neck

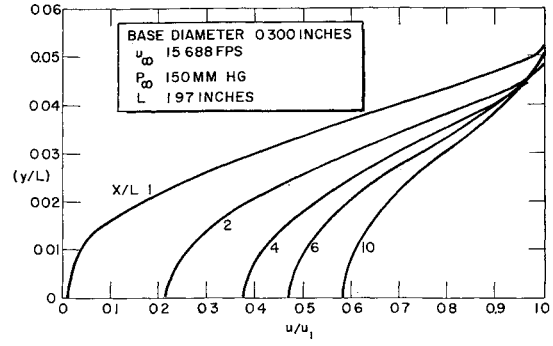

Fig 2 Velocity profiles in the equilibrium wake of a 10° cone

of the near wake, the Crocco integral will be used in the present analysis to specify the initial total enthalpy

Assuming, a priori, that the net drag contribution of the near wake is negligible in comparison with that shed from the body in the boundary layer, the initial momentum thickness is given by

$$[\rho_1 u_1^2 \theta^{j+1}]_{\text{neck}} = [\rho_1 u_1^2 d^j \theta]_{\text{body}}$$

where

$$\theta_{\text{neck}} = \left\{(j+1)\int_0^\delta \frac{\rho u}{\rho_1 u_1}\left(1-\frac{u}{u_1}\right) r^j dr\right\}^{1/(j+1)}_{\text{neck}}$$

$$\theta_{\text{body}} = \left\{\int_0^\delta \frac{\rho u}{\rho_1 u_1}\left(1-\frac{u}{u_1}\right) dy\right\}_{\text{body}}$$

In the numerical examples, the initial value of the thickness parameter λ is computed from the neck momentum thickness in the following manner:

$$\lambda = (\theta_{\text{neck}}/L)^2 \{Re_L/(j+1)F_{1_1}\}^{2/(j+1)}$$

The preceding assumptions are verified a posteriori only in that they lead to results that are in good agreement with the experimentally observed facts (i e , the wake thickness and its Reynolds number dependence), which are discussed in greater detail later in this paper However, when they are applied at very low pressures (high altitude) certain anomalous results are obtained, namely initial wake thicknesses, which exceed the body diameter and even the "displaced" body diameter (i e , body plus boundary layer) This is undoubtedly due to neglect of interaction with the inviscid flow The viscous-inviscid interaction is a separate problem which is not considered in this analysis nor in any of the examples

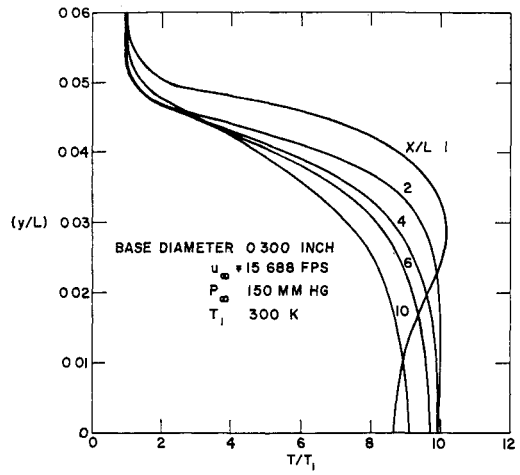

Fig 3 Temperature profiles in the equilibrium wake of a 10° cone

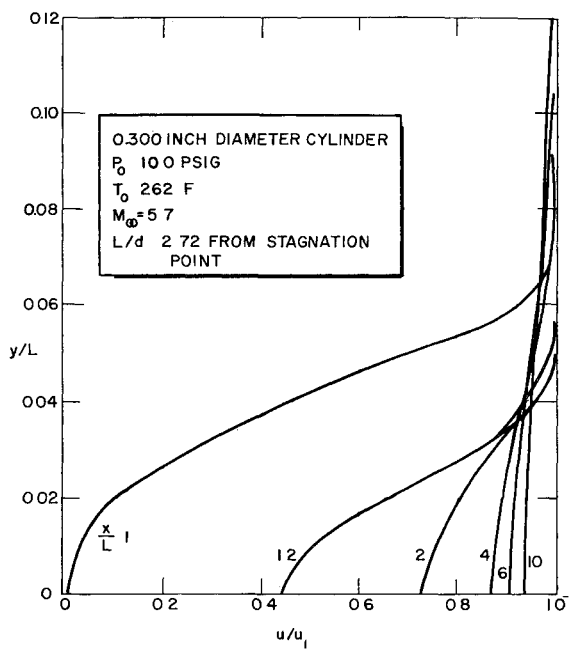

Fig 4 Velocity profiles in the wake of a cylinder

B Numerical Examples‡‡

The present analysis was applied to study the development of the laminar far wake for some typical cases of interest The medium is assumed to be air in equilibrium, unless otherwise noted, with a constant Prandtl number of 0 72

The following case is an example for which conditions are typical of experiments performed in the Avco/RAD ballistics range: 10° (semivertex angle) cone; base diameter, 0 300 in ; velocity, 15,688 fps; pressure, 150 mm Hg The axial pressure gradient is neglected on the basis of method of characteristics solutions for this and other slender bodies Velocity and temperature profiles (with $H_e/H_1 = 0\,3$ initially)

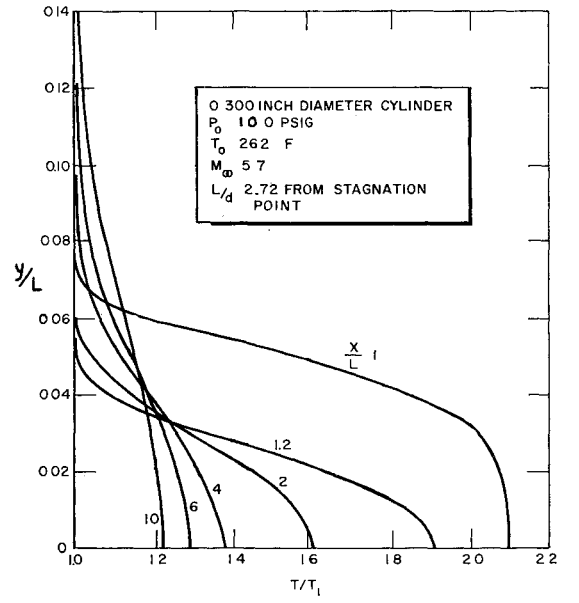

Fig 5 Temperature profiles in the wake of cylinder

‡‡ In all the numerical examples presented herein, six strips were used in the computations Rapid convergence of the results was obtained with $N \geq 4$ Computer time of about 5 to 10 min/case (on an IBM 7094) is required, with $N = 6$, to approach the known asymptotic solution[6] (i e , to reach a small velocity defect)

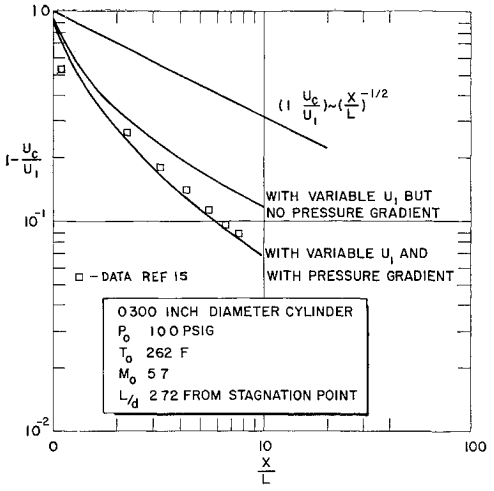

Fig 6 Velocity decay in the wake of a cylinder

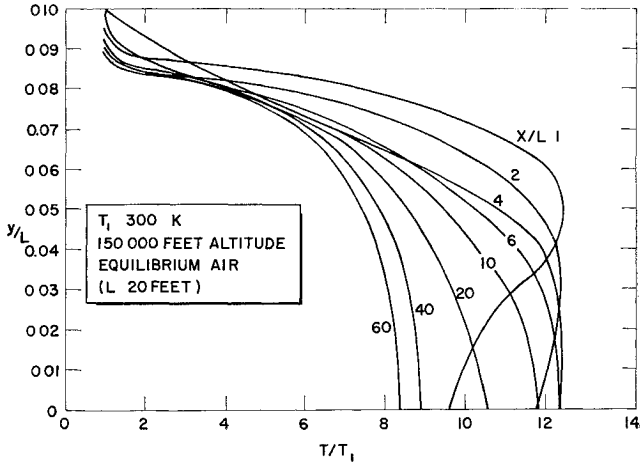

Fig 8 Temperature profiles for a 10-ft 12° cone

for the wake at these conditions are shown in Figs 2 and 3 The features of the flow field which can be observed from the schlieren photos (e g , Fig 1, the thickness and growth rate) are, essentially, in agreement with these results

This slender, axisymmetric body example is now contrasted to the results for a blunt semi-infinite body; namely, a cylinder placed normal to the flow The conditions selected correspond to one of the experiments performed by McCarthy in the Graduate Aeronautical Laboratories, California Institute of Technology (GALCIT) wind tunnel[15]: 0 300-in -diam cylinder; freestream Mach number, 5 7; reservoir pressure, 10 psig; reservoir temperature, 262°F In this case, the viscous core may entrain mass flow from the entropy layer as it grows This "swallowing" effect was estimated using the method of characteristics It was found, however, that the laminar core (in the present example) does not entrain any appreciable mass from the entropy layer for at least 25 diam from the neck An appreciable velocity gradient is encountered, none-the-less, due to the presence of expansion waves reflected from the bow shock §§

A constant stagnation enthalpy (equal to the freestream value) was assumed, since the tunnel running time was long, allowing the model to approach an equilibrium temperature Because of the low static temperature, the medium was assumed to be a perfect gas Typical resulting velocity and temperature profiles are shown in Figs 4 and 5 The very fast velocity decay observed here is similar to that found in the classical flat-plate solution and appears to be peculiar to semi-infinite bodies The relative importance of the nonsimilar behavior of the solution and also of the attendant favorable pressure gradient in this example are illustrated in Fig 6 As much as a 70% error in velocity defect (however, this is less than 1% of u_1) can be attributed to neglect of the pressure gradient It should also be noted that no effect of Reynolds number on the decay rates can be expected if the initial value of the thickness parameter λ is constant, which is consistnt with McCarthy's data

As an example for the laminar far wake of a full-scale slender body at flight conditions, a constant velocity (22,000 fps) trajectory from 200,000 to 100,000 ft was assumed for a 10-ft, 12° (semivertex) angle cone An initial enthalpy ratio of $H/H_1 = 0\,3$ was assumed, and any axial pressure gradient was neglected Typical profiles of velocity and temperature are given in Figs 7 and 8 for an altitude of 150,000 ft The velocity and stagnation enthalpy decay along the axis is shown in Fig 9 The results at other altitudes are qualitatively similar However, it is interesting to note that the length of the trail is found to grow with decreasing altitude [16]

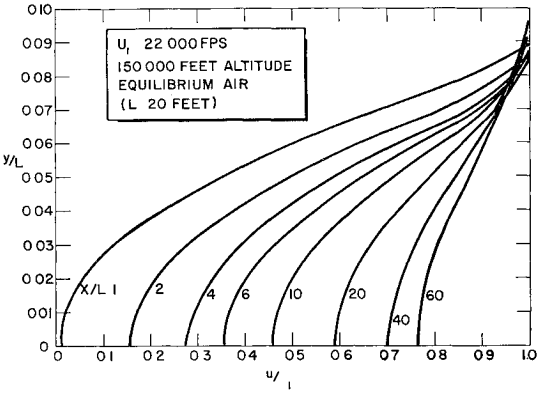

Fig 7 Velocity profiles for a 10-ft 12° cone

IV Experimental Studies

A series of ballistic-range experiments with conical models of 10°, 15°, and 27½° half-angles were performed The model velocities range between 4000 and 17,000 fps with range pressures varying from 15 to 380 mm of Hg in air

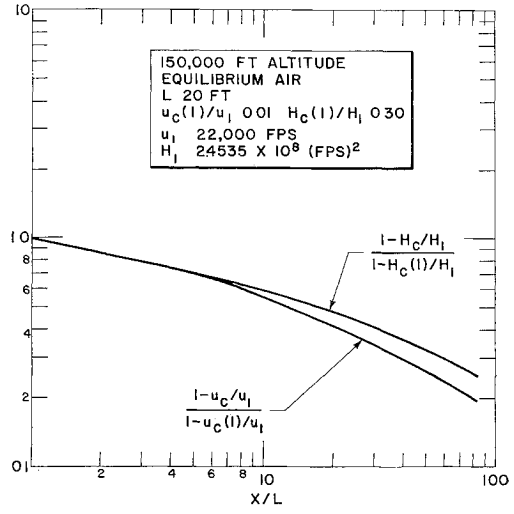

Fig 9 Velocity and enthalpy decay along the wake axis for a 10-ft 12° cone

§§ Attention must be called to the fact that any streamwise pressure gradients generated in the inviscid flow field of a slender, sharp cone are much smaller than those encountered with a blunt body and are usually negligible Possible exceptions may be found only in the near wake and immediate vicinity of the neck

Table 1 Summary of experimental conditions and transition data from ballistic range

ϕ, deg	d in	$V_\infty \times 10^{-3}$, fps	P_∞, mm Hg	M_1	$(Re/\text{ft})_1$ $\times 10^{-6}$	$(T_c/T_1)_{n\ k}$ [a]	Re_{x_t} $\times 10^{-6}$	ξ_t	$\bar{M}_{1t}$ [a]	$(T_c/T_1)_t$ [a]
10	0 3	10 0	50	8 8	4 6	4 5	2 5	3 3	5 0	5 9
10	0 3	9 7	75	8 5	6 9	4 4	2 7	2 3	5 9	5 9
10	0 3	9 3	40	8 1	3 4	4 0	0 99	3 3	4 4	5 1
10	0 3	10 0	40	8 8	3 7	4 5	1 7	2 7	5 3	6 0
10	0 3	9 5	100	8 3	8 8	4 5	2 7	1 8	6 5	6 1
10	0 3	9 0	350	7 9	30 0	3 8	5 5	1 0	7 9	3 8
10	0 3	4 9	150	4 3	6 8	1 4	1 0	1 0	4 3	1 4
10	0 3	11 7	150	10 3	17 0	6 0	3 6	1 4	9 0	7 3
10	0 3	13 0	150	11 6	19 0	8 3	6 8	2 1	8 6	11 5
10	0 3	14 8	150	13 0	21 0	8 3	5 6	1 8	10 5	9 6
10	0 3	15 7	150	13 6	21 0	8 7	15 0	2 3	10 2	10 0
10	0 3	14 1	100	12 5	14 0	8 0	5 3	2 3	8 7	9 4
15	0 4	8 1	75	7 1	5 6	3 2	2 1	2 3	5 4	4 3
15	0 4	10 0	75	8 7	6 7	4 5	1 7	1 6	7 5	5 6
15	0 4	12 7	75	10 6	7 2	6 2	2 7	2 3	8 1	7 5
15	0 4	10 5	30	9 2	2 9	4 9	1 7	3 6	4 7	6 1
15	0 4	9 6	100	8 4	8 8	4 2	2 1	1 5	7 4	5 2
15	0 4	10 3	100	9 0	9 6	4 8	2 2	1 4	8 0	5 8
15	0 4	9 0	150	7 9	12 0	3 8	2 6	1 3	7 2	4 4
15	0 4	9 8	250	8 6	23 0	4 7	5 1	1 2	8 2	5 3
15	0 4	13 3	100	10 8	8 8	6 2	3 2	2 3	8 4	7 4
15	0 4	14 5	100	12 2	11 0	7 4	5 6	2 8	9 0	8 6
15	0 3	14 2	150	11 8	16 0	7 1	3 9	2 0	9 6	8 2
15	0 3	14 6	100	12 0	10 0	7 2	3 7	2 3	9 3	8 3
15	0 3	15 8	100	12 9	11 0	7 6	4 1	2 6	9 4	8 8
15	0 3	10 0	360	8 8	33 0	4 5	4 3	1 0	8 7	4 5
27 5	0 3	9 2	50	5 5	1 2	2 1	0 36	3 5	3 3	2 9
8 [b]	0 4	14 8	100	13 0	13 0	8 3	6 1	2 1	10 7	9 5
8 [b]	0 4	14 8	100	13 0	13 0	8 3	9 0	3 1	9 7	9 6

[a] Computed for equilibrium air with $H/H_1 = 0\,3$ and $u/u_1 = 0\,01$
[b] From Naval Ordnance Laboratory

The techniques for the use of a light-gas gun for launching projectiles to re-entry velocities are well established A conical model (with semivertex angles between 10° and 20°) has been developed which can achieve velocities up to 17,000 fps while withstanding the launching environment of a light-gas gun This model is fabricated with a steel tip and titanium afterbody, and has a hollow base to provide a static margin of 15% ¶¶ A one-piece steel cone model (having a hollow base) has been used for half-angles of 27 5°

Two 0 600 caliber light-gas gun ranges have been used in this program * The first range is equipped with a 12-in -diam double-traverse schlieren system The 12-in -diam parabolic mirror is located inside a 10-ft diam by a 14-ft-long tank This range has been used to study the low-velocity regime (under 11,000 fps) where the sensitivity of the double-traverse system is utilized for flow visualization at low density (e g , pressures in the range $15 < P < 100$ mm Hg) A second caliber 0 600 light-gas gun range has been used to obtain data from 11,000 to 17,000 fps at pressures greater than 30 mm Hg in air Primary instrumentation on this range is a 12-in -diam single-pass schlieren apparatus

Some results covering the range of experimental conditions for which transition was clearly observable from the schlieren photographs are compiled in Table 1 Four of the schlieren photographs which exemplify the typical features of the flow field of a slender body wake are presented here as Figs 1 and 10–12 Similar features can be seen in shadowgraph photos (e g , Ref 5, Fig 1) It should be noted that present visualization techniques are inadequate at these pressures and velocities to provide near-wake details Rather, recourse must be made to observables such as the apparent origin of the trailing shock and/or a minimum thicknes section to define the neck location

Model pitching in the plane of the photograph is clearly identifiable by the asymmetric location of the wake within the shock layer Small yaw angles normal to the plane of the photograph are indicated by an abnormally thick wake as compared to zero yaw at the same conditions, and by appearance of a streak down the center of the wake

The occurrence of turbulence is always clearly identifiable for sharp bodies† and is usually preceded by an instability which manifests itself as sinusoidal waviness of the wake Generally, the waviness is almost immediately followed by turbulence, but occasionally it persists for an appreciable length before breakdown into turbulence In none of the photos does the wake appear to be pulsing (i e , periodically changing diameter); however, some evidence of helical motion can be seen in the cases with yaw The effect of pressure on transition is demonstrated in Figs 1, 10, and 11; the effect of velocity can be inferred from Figs 1 and 12 where the transition distance is held constant (regardless of doubling the pressure) by increasing the model velocity

V Transition Correlation

It is generally agreed that wake transition is dependent on a Reynolds number and a Mach number which are based on the relative velocity of the wake $u_1 - u$ (e g , Refs 4 and 17–20) Stability theory for compressible flows indicates that the Reynolds number and Mach number should be evaluated using physical properties at the "critical point" in the layer [20] However, transition correlations commonly use properties at the outer edge of the layer and introduce a temperature ratio as a third parameter Several length scales, namely surface distance to transition point, boundary-

¶¶ The hollow base may alter the base flow and near-wake structure to some extent, but presumably any influence on the far wake is negligible No solid base models have been flown successfully

* A description of the Avco/RAD ballistics range facility and these tests is summarized in Ref 16

† This is not necessarily the case for blunt bodies where the viscous core may be obscured by the inviscid entropy layer that enshrouds it

layer thickness, momentum thickness, etc , have been employed in defining a transition Reynolds number None of these parameters is completely satisfactory in situations where the viscous layer history is significant (e g , strongly varying edge properties, nonsimilar profile shape, etc)

Clearly, the latter remarks are appropriate to wake transition A heuristic approach to this problem (short of a complete stability analysis) is to attempt correlation using a physically reasonable length scale, such as that from the origin of the viscous layer to the transition point X_t, or the wake diameter at transition δ_t, both of which are readily measurable A third possibility, however, is the relative distance‡ a particle travels along the axis to the transition point $\bar{X}_t$ This is a measure of the time which a disturbance that is convected with the particle has to amplify The significance of this time is suggested by the experiments of Sato and Kuriki[21] in which the disturbances were observed to originate at the center of the wake and grow as they convected downstream

Some discussion of these parameters (in particular the last) and results of correlations based on all three are offerred in Ref 16 The present data is found to correlate well in terms of δ_t and $\bar{X}_t$ Since the latter is quite cumbersome

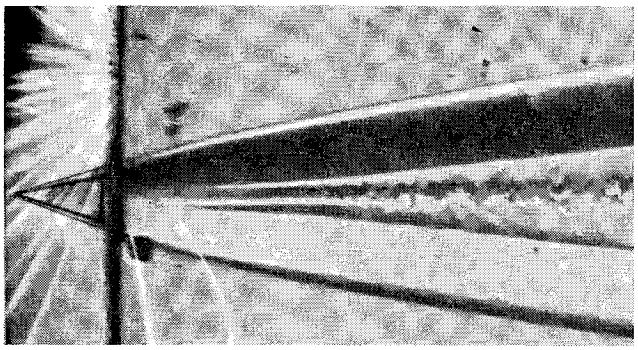

Fig 10 Typical features of a slender body flow field (15 cone, V_∞ = 10,000 fps, 0 400-in base diameter, P_∞ = 250 mm Hg)

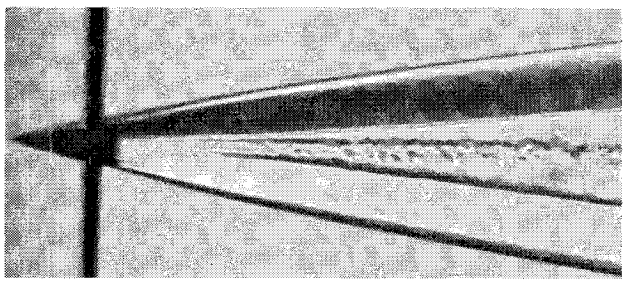

Fig 11 Typical features of a slender body flow field (10° cone, V_∞ = 9000 fps, 0 300-in base diameter, P_∞ = 350 mm Hg)

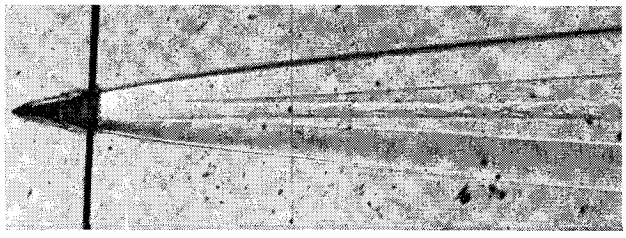

Fig 12 Typical features of a slender body flow field (10° cone, V_∞ = 15,700 fps, 0 300-in base diameter, P_∞ = 150 mm Hg)

‡ i e , in a coordinate system fixed with respect to the medium in which the body is immersed

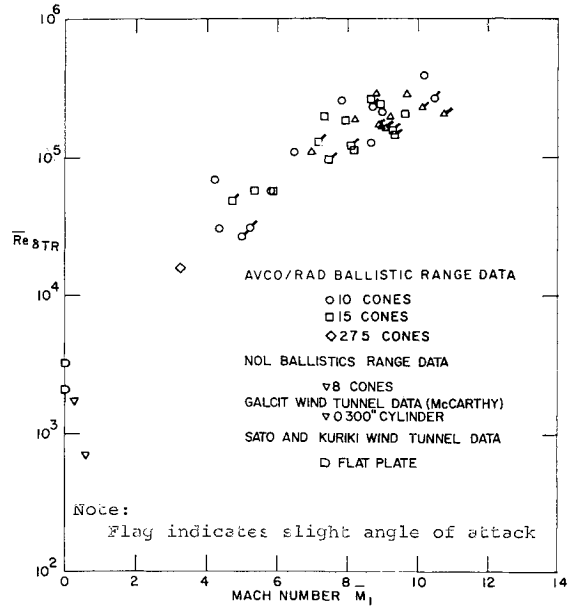

Fig 13 Wake transition correlation (based on measured wake diameter)

to compute and has no apparent advantage over the former in correlating the data, only the correlation based on the wake diameter at transition is considered here

Utilizing the values of X_t and δ_t measured from photographs§ and values of u/u_1 computed by the present (6-strip) method, the experimental data from the Avco/RAD and NOL ballistic ranges, and also some wind-tunnel data from Refs 15 and 21, are correlated in Fig 13 where

$$\bar{M}_1 = (u_1/a_1)[1 - (u/u_1)]$$

$$\overline{Re}_\delta = (\rho_1 u_1 \delta/\mu_1)[1 - (u_c/u_1)]$$

The scatter in this correlation is at least partially due to the fact that no attempt to account for temperature effects has been included The ratio of T/T_1 at transition ranges from about 4 to 10 for the slender cones at high velocity, based on the assumed value of H/H_1 = 0 3 at the neck (From Table 1, the value of T/T_1 at transition for case 7 is given as 1 4 However, the assumption that H/H_1 = 0 3 is probably inconsistent with the low velocity of this case) In the experiments of Sato and Kuriki the temperature ratio was, of course, unity, and in McCarthy's experiments the ratio was about 1 5

VI Prediction of Transition

The $\overline{Re}_\delta$ and $\bar{M}_1$ histories of the wakes of 5-, 10-, and 15-ft 12° cones have been computed and are shown in Fig 14 ¶ The intersection of these curves with a mean line through the correlation of Fig 13 is interpreted as defining the loci of transition points in the wake Presumably, the transition Reynolds number for the boundary layer will also increase with Mach number (although present data[22 23] are insufficient to be conclusive) inferring that transition on the cone surface will occur in the neighborhood of 100,000 ft, at which time

§ The location of transition was defined from photographs by the occurrence of distinct and continuous "waviness" of the wake It is not clear that this is consistent with other experimental techniques for defining transition or instability (e g , Refs 15 and 21)

¶ A constant velocity (22,000 fps) trajectory between 200,000 and 100,000 ft is assumed The thickness δ computed from the analysis is the wake radius and is doubled to correspond to the measured wake diameter

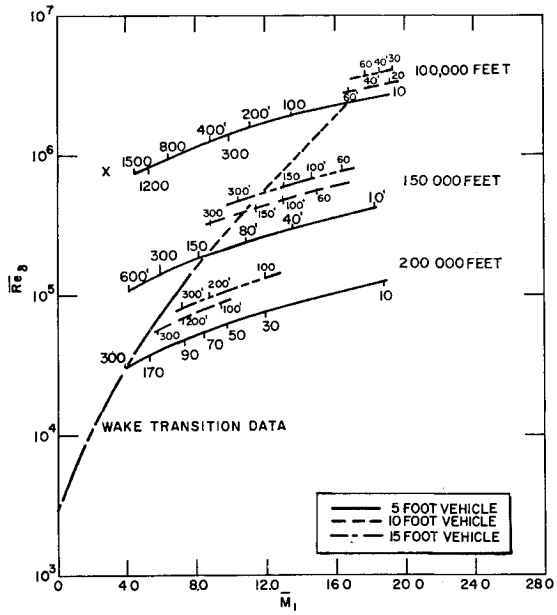

Fig 14 Wake transition for a 12° cone at 22,000 fps based on R

the near wake and any portion of the far wake still laminar would be tripped **

The effects of chemical nonequilibrium on the prediction of transition have not been considered explicitely The velocity decay is coupled to the energy equation only through the $\rho\mu$ ratio and the density, both of which are only weakly influenced as functions of enthalpy by dissociation and relaxation Hence it is anticipated that transition will be only slightly affected by chemical nonequilibrium

It should be noted that in the downstream (asymptotic) limit, $\overline{Re}_\delta \sim X^{-1/2}$ for axisymmetrc flow and $\overline{Re}_\delta \sim$ const for planar flow In either case, at a sufficiently low pressure or high altitude, a completely laminar wake regardless of the value of X is implied by the minimum value of $(\overline{Re})_{\delta tr}$ at $\overline{M}_1 = 0$

VII Neck Thickness of the Laminar Wake

As in the previous discussion (Sec III) on the momentum thickness at the neck, it may be shown that the over-all wake thickness at the neck must also vary as the square root of the boundary-layer thickness for an axisymmetric body, as opposed to a linear relation in the planar (semi-infinite) case In particular, if negligible net mass addition to the viscous core in the near-wake region is assumed, then a simple mass balance yields

$$\left[\rho_1 u_1 \delta^{j+1}\left(1 - \frac{\delta^{*j+1}}{\delta^{j+1}}\right)\right]_{\text{neck}} = \left[\rho_1 u_1 d^j \delta\left(1 - \frac{\delta^*}{\delta}\right)\right]_{\text{body}}$$

where

$$\delta^*_{\text{neck}} = \left\{(j+1)\int_0^\delta \left(1 - \frac{\rho u}{\rho_1 u_1}\right) r^j dr\right\}^{1/(j+1)}_{\text{neck}}$$

$$\delta^*_{\text{body}} = \left\{\int_0^\delta \left(1 - \frac{\rho u}{\rho_1 u_1}\right) dy\right\}_{\text{body}}$$

** It is anticipated that surface ablation will have two opposing effects on the boundary-layer stability The blowing itself tends to be destabilizing but, on the other hand, it will enhance the stablizing effect due to the flavorable pressure gradient (induced by viscous inviscid interaction) by further increasing the displacement thickness

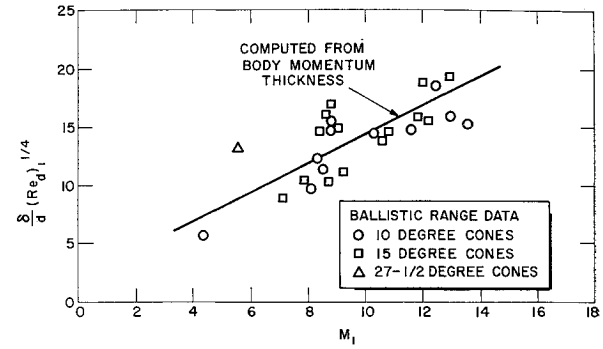

Fig 15 Laminar wake thickness at the neck for sharp cones

For a slender cone this can be reduced to

$$\left[\frac{\delta}{d}(Re_d)^{1/4}\right]_{\text{neck}} = \left[\frac{(\rho_1 u_1 \mu_1)_{\text{cone}}}{(\rho_1 u_1 \mu_1)_{\text{neck}}}\left(\frac{1}{2\sin\phi}\right)\right]^{1/4} f(M_\infty, Tw, \phi)$$

$$\approx \left[\frac{P_{\text{cone}}/P_\infty}{2\sin\phi}\right]^{1/4} f(M_\infty, Y_w, \phi)$$

$$\approx \left(\frac{\gamma}{2} M_\infty\right)^{1/4} f(M_\infty, T_w, \phi)$$

where

$$f(M_\infty, T_w, \phi) = \left\{\frac{\{(\delta/L)(Re_L)^{1/2}[1 - (\delta^*/\delta)]\}_{\text{cone}}}{[1 - (\delta^*/\delta)^2]_{\text{neck}}}\right\}^{1/2}$$

The parameter $[(\delta/d)(Re_d)^{1/4}]_{\text{neck}}$ was found to be essentially a function solely of Mach number for the range of cone angle and Mach number combinations encountered in the present tests when computed in the manner discussed in the previous section on initial conditions (i e , employing the values of δ which give the proper drag at the neck when used with the assumed separation point velocity profile) The values of this parameter based on the experimentally measured neck thickness are shown in Fig 15 to compare remarkably well with the computed curve ††

VIII Conclusions

A nonsimilar, integral solution of the governing equations for the laminar far wake has been formulated for equilibrium air or a frozen gas Some numerical examples are presented, using the present analysis, which emphasize the nonsimilar behavior near the neck of the wake Similarity (linearized) solutions for the wake, which are appropriate only asymptotically (i e , for very small velocity defect), are particularly inaccurate for the wake of a slender axisymmetric body at hypersonic speeds which is shown to generate a large velocity defect which persists far behind the body

A series of ballistic range experiments on slender cones in the Avco/RAD facilities are summarized and the results discussed The preceding analysis is used to compute appropriate parameters for the correlation of wake transition and neck diameter from these data Moreover, predictions of wake transition for a 12° half-angle cone at 22,000 fps are made which indicate that transition moves from about 300 ft behind the cone apex at an altitude of 200,000 ft to about 30 ft at 100,000 ft, for a 5-ft-long cone, for example Increasing the cone length to 15 ft is shown to add about 100 ft to the length of the laminar trail at 200,000 ft and to add about 10 ft at 100,000 ft It is not anticipated that a nonequilibrium state of the air will significantly alter these results The existence of an altitude above which transition never occurs (for a given vehicle and velocity) is also indicated by the correlation

†† The thickness δ in this figure is the wake diameter rather than radius

References

[1] Feldman, S, On trails of axisymmetric hypersonic blunt bodies flying through the atmosphere,' J Aerospace Sci **28,** 433–448 (1961)

[2] Lees L and Hromas L, 'Turbulent diffusion in the wake of a blunt-nosed body at hypersonic speeds J Aerospace Sci **29,** 976–993 (1962)

[3] Vaglio Laurin R and Bloom, M, Chemical effects in ex ternal hypersonic flows," *ARS Progress in Astronautics and Rocketry: Hypersonic Flow Research* edited by F R Riddell (Academic Press Inc, New York, 1962), Vol 7, pp 205–254

[4] Lees, L, "Hypersonic wakes and trails," ARS Preprint 2662-62 (November 13–18, 1962)

[5] Vaglio-Laurin, R, Bloom, M H, and Byrne R W, ' Aero physical aspects of slender body re entry, ARS Preprint 2674-62 (November 13–18, 1962)

[6] Goldstein, S, *Modern Developments in Fluid Dynamics* (Oxford University Press, London 1938), Vol 2, pp 571–574; also Schlicting, H, *Boundary Layer Theory* (McGraw-Hill Book Co, Inc, New York, 1955), pp 138–142

[7] Pallone A "Nonsimilar solutions of the compressible laminar boundary layer equations with applications to the upstream-transpiration problem" J Aerospace Sci **28,** 450–456 (1961)

[8] Bloom, M H and Steiger, M H, "Diffusion and chemical relaxation in free mixing' IAS Paper 63 67 (January 21-23, 1963)

[9] Lien, H, Erdos, J, and Pallone, A, "Nonequilibrium wakes with laminar and turbulent transport," AIAA Preprint 63-447 (August 26–28, 1963)

[10] Pallone, A, Moore, J, and Erdos, J, ' Nonequilibrium, nonsimilar solutions of the laminar boundary layer equations," AIAA Preprint 64 40 (January 20–22 1964)

[11] Katz, I, Morrissette, L, and Warga, J, "A space trajectory program," Avco/RAD TM-61-10, Sec III (May 2, 1961)

[12] Denison M R and Baum E, "Compressible free shear layer with finite initial thickness," IAS Paper 62-125 (June 19–22, 1962)

[13] Chapman, D R, Kuehn, D M, and Larson, H K, "Investigation of separated flows in supersonic and subsonic streams with emphasis on the effect of transition," NACA Rept 1356 (1958)

[14] Cohen, C and Reshotko, E, ' Similar solutions for the compressible laminar boundary layer with heat transfer and pressure gradient,' NACA TN 3325 (February 1955)

[15] McCarthy, J F, "Hypersonic wakes,' Graduate Aeronautical Labs, California Institute of Technology Hypersonic Research Project Memo 67 (July 1962); also AIAA Preprint 63-170 (June 17, 1963)

[16] Pallone, A, Erdos, J, Eckerman J, and McKay, W, "Hypersonic laminar wakes and transition studies" Avco/RAD TM-63-33 (June 1963); also AIAA Preprint 63-171 (June 17, 1963)

[17] Webb, W, Hromas, L, and Lees, L, "Hypersonic wake transition," AIAA J **1,** 719–721 (1963)

[18] Lin, C C, *Theory of Hydrodynamic Stability* (Cambridge University Press Cambridge, England 1955), p 120

[19] Pai, S, "On the stability of two dimensional laminar jet flow of gas," J Aeronaut Sci **18,** 731–742 (1951)

[20] Gold, H, "Stability of laminar wakes, PhD Thesis, California Institute of Technology (1963)

[21] Sato, H and Kuriki, K, ' The mechanism of transition in the wake of a thin flat plate placed parallel to a uniform flow," J Fluid Mech **11,** 321–352 (November 1961)

[22] Czarnecki, K and Jackson, M, "Effects of nose angle and Mach number on transition on cones at supersonic speeds," NACA TN 4388 (September 1958)

[23] Schueler, C, "A comparison of transition Reynolds numbers from 12 and 40-inch supersonic tunnels,' Arnold Engineering Development Center-TDR-63-57 (March 1963)

[24] Kubota T, private communication (June 1963)

[25] Cheng S I "Flow around an isolated stagnation point in the near wake," Avco/RAD TM-63-23 (April 25, 1963)